AD-A116 450 PURDUE UNIV LAFAYETTE IN DEPT OF CHEMISTRY F/G 7/4
INSTRUMENTATION AND METHODOLOGY FOR GENERATION OF AN ELECTROCHE--ETC(U)
MAY 82 W A BYERS, S P PERONE N00014-75-C-0674
UNCLASSIFIED TR-27 NL

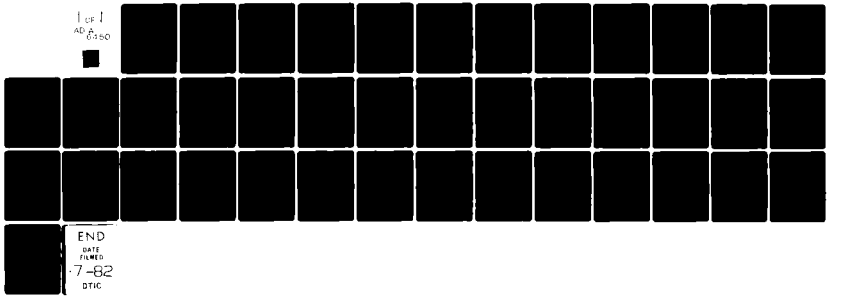

(12)

OFFICE OF NAVAL RESEARCH

Contract No. N00014-75-C-0874

Task No. NR 051-552

TECHNICAL REPORT NO. 27

Instrumentation and Methodology for Generation of an Electrochemical Data Base for Pattern Recognition

by

W. Arthur Byers[a] and S. P. Perone*[b]

Department of Chemistry
Purdue University
W. Lafayette, IN 47907

Prepared for Publication in

Analytical Chemistry

May, 1982

(a) Present address: Westinghouse Electric Corporation
1310 Beulah Road
Pittsburgh, PA 15235

(b) Present address: Chemistry & Materials Science Department
Lawrence Livermore National Laboratory
P.O. Box 808, L-326
Livermore, California 94550

SECURITY CLASSIFICATION OF THIS PAGE (When Data Entered)

REPORT DOCUMENTATION PAGE		READ INSTRUCTIONS BEFORE COMPLETING FORM
1. REPORT NUMBER Technical Report No. 27	2. GOVT ACCESSION NO. AD-A116 450	3. RECIPIENT'S CATALOG NUMBER
4. TITLE (and Subtitle) Instrumentation and Methodology for Generation of an Electrochemical Data Base for Pattern Recognition		5. TYPE OF REPORT & PERIOD COVERED Interim 6. PERFORMING ORG. REPORT NUMBER
7. AUTHOR(s) W. Arthur Byers and S. P. Perone		8. CONTRACT OR GRANT NUMBER(s) N00014-75-C-0874
9. PERFORMING ORGANIZATION NAME AND ADDRESS Purdue University Department of Chemistry W. Lafayette, IN 47907		10. PROGRAM ELEMENT, PROJECT, TASK AREA & WORK UNIT NUMBERS NR 051-552
11. CONTROLLING OFFICE NAME AND ADDRESS Materials Science Division Office of Naval Research Arlington, VA 22217		12. REPORT DATE May, 1982 13. NUMBER OF PAGES 33
14. MONITORING AGENCY NAME & ADDRESS(if different from Controlling Office)		15. SECURITY CLASS. (of this report) Unclassified 15a. DECLASSIFICATION/DOWNGRADING SCHEDULE

16. DISTRIBUTION STATEMENT (of this Report)

Approved for Public Release, Distribution Unlimited

17. DISTRIBUTION STATEMENT (of the abstract entered in Block 20, if different from Report)

18. SUPPLEMENTARY NOTES

Submitted for publication in Analytical Chemistry

19. KEY WORDS (Continue on reverse side if necessary and identify by block number)

pattern recognition
factorial design
instrumentation voltammetry
electrochemistry
differential capacity
electrochemical data base

20. ABSTRACT (Continue on reverse side if necessary and identify by block number)

Instrumentation and methods are presented for determining the Faradaic and capacitive responses of an analyte over a wide range of experimental conditions. Experiments were carried out by a fractional factorial design so that the best experimental conditions or changes in conditions for analyte identification could be determined in a later pattern recognition analysis. Percent ethanol, pH, surfactant concentration, number of cycles, scan rate, and mercury drop hang time all produced changes in cyclic differential capacity curves and

DD FORM 1 JAN 73 1473 EDITION OF 1 NOV 65 IS OBSOLETE
S/N 0102-014-6601

SECURITY CLASSIFICATION OF THIS PAGE (When Data Entered)

cyclic staircase voltammograms which were unique and reproducible. Capacitive and Faradaic responses were determined independently for 19 nitrocompounds under most experimental conditions.

BRIEF

Instrumentation and methods are presented for determining the Faradaic and capacitive responses of an analyte over a wide range of experimental conditions. The goal of this work is the generation of an electrochemical data base containing a large amount of structural information which can be used to classify organics in a later pattern recognition analysis.

ABSTRACT

Instrumentation and methods are presented for determining the Faradaic and capacitive responses of an analyte over a wide range of experimental conditions. Experiments were carried out by a fractional factorial design so that the best experimental conditions or changes in conditions for analyte identification could be determined in a later pattern recognition analysis. Percent ethanol, pH, surfactant concentration, number of cycles, scan rate, and mercury drop hang time all produced changes in cyclic differential capacity curves and cyclic staircase voltammograms which were unique and reproducible. Capacitive and Faradaic responses were determined independently for 19 nitrocompounds under most experimental conditions.

Electroanalytical techniques have not often been used for elucidation of chemical structure. This is due in part to the fact that normally recorded organic electrochemical responses are usually complex functions of many variables such as electrode material, solution composition and the time frame of the experiment. Theoretical expressions relating structure to electrochemical activity are valid under very restrictive conditions (1), and they are often difficult to evaluate (2, 3, 4).

An empirical approach such as computerized pattern recognition would seem to be the best solution for qualitative identification, and it has already been used with some success in electrochemistry (5, 6, 7, 8). However, in order to use pattern recognition to assign an unknown to a specific structural class, one must first have a library of data for similar structures, obtained under conditions similar to those for the unknown. Although a vast amount of organic electrochemical data has been collected (9), only small subsets have been collected under conditions which are sufficiently similar for a pattern recognition analysis. Burgard and Perone (10) reported encouraging results for the analysis of 30 organics representing four structural classes, but better results might have been obtained if solution conditions had been varied.

Much of the complexity of an electrochemical response is due to the heterogeneous nature of the electron transfer. The interplay of adsorption and diffusion complicate the interpretation of current flowing due to electron transfer. It is common practice to use a solvent system such that adsorption effects are minimized. While this may improve peak shape for more accurate quantitation, one may be throwing away important structural information in the process. The strength and potential dependence of adsorption may indicate the presence of certain functional groups (12, 13). π-electron interaction has a characteristic influence on the adsorption behavior of organics (14), and specific interactions between the analyte and some other molecule or ion within the double layer may also be helpful in identification (15, 16). For these reasons we believe that structural classifications might be made more reliably by using solution conditions where adsorption strongly affects electrochemical response.

The purpose of this work is to describe new methods and instrumentation which we have developed for producing a large body of electrochemical data and for determining the best measurements to be made for later pattern recognition analysis. The effects of seven different experimental variables on Faradaic and capacitive electrochemical responses have been examined. Initial results for several nitrodephenylethers are reported and compared to other nitroaromatics. These compounds are important in agriculture because of their strong but selective herbicidal activity (11).

Electrode capacitance is related in a simple way to the degree of adsorption or surface excess (17). A number of methods are available

for simultaneous recording of capacitive and Faradaic responses (18-22), one of the best having been recently reported by Elkin et al. (23). Elkin's semitrapazoidal waveform (Figure 1a) is optimal in terms of potentiostat stability, but is difficult to generate experimentally. We have found that a simple staircase (Figure 1b) will produce excellent results while being easy to generate under computer control. Electrode capacitance is obtained by measuring the rate of charging current decay immediately after the step. The advantages of making Faradaic measurements with staircase voltammetry have been enumerated elewhere (24, 25).

EXPERIMENTAL

Experimental Design

The seven variables which were investigated are listed in Table 1. Performing a series of experiments in which one parameter is varied while all others are held constant at some arbitrary level would give a very narrow view of the effects of each parameter if there was any possibility of interaction between variables. To get a broader view of each variable effect, the experiments were conducted by a fractional factorial design (26). Two saturated fractions were run so that all main effects were de-aliased from two-factor interactions (27). Higher order interactions could still be confused with the main effects, but in most cases, such interactions are relatively small in magnitude. The level of each variable in the 16 experiments is given in Table 2. One experiment, #5, was repeated to test for reproducibility.

The main effects were explored with the aid of variable effect curves. These curves were constructed for each variable by summing point-by-point all responses obtained for those experiments in Table 2 where the variable was at its high level, and then subtracting all responses where the variable was at its low level. This approach is analogous to the method reported in Ref. 26 for extracting the contribution of each variable, free from the effects of other variables. Effect curves were plotted for both the Faradaic and capacitive responses.

Solution Preparation

Compounds analyzed in this study are listed in Table 3. The diphenylethers were gifts from Dr. F. D. Hess, Department of Botany and Plant Pathology, Purdue University. Purity was 95% or better. Other compounds were commercially available in pure form. Stock solutions were 2.0×10^{-3} M and were made by dissolving the compounds in 2.5 ml. of ethanol and diluting to 50 ml. with distilled water. The final concentration was 1.6×10^{-4} M after complete solution preparation.

Britton-Robinson buffers were used for pH control. These were made by adding reagent grade boric acid, sodium acetate, dibasic potassium phosphate and potassium chloride to either distilled, deionized water or to a 10% ethanol solution so that each of the components was 0.02 F. The stock buffer solutions were stored in 5 gallon carboys and were delivered to the cell via de-oxygenating columns and automatic pipettes shown in Figure 2. The aqueous buffer was continuously irradiated with U.V. light to prevent the growth of bacteria. Purified nitrogen was used for deoxygenation. Stainless steel A.C. solenoid valves (ALCO 204CA1/453/32G) controlled the flow of solution through the pipettes. The volume of solution delivered was set to 46.0 ml. by adjusting the position of the pipettes relative to the cell entry port. The standard deviation for 3 successive deliveries was found to be 0.02 ml.

Sodium lauryl sulfate, 1.85 M nitric acid and the analyte were delivered to the cell by a Technicon Proportioning Pump (Model III) and latching 3-way solenoid valves. The sodium lauryl sulfate solution was 10^{-3} M and contained a mixture of alkyl sulfates, lauryl sulfate

being the primary species. The valve used for control of the nitric acid flow was constructed from Teflon (General Valve 1-36) while the others were stainless steel (Angar Scientific Corporation, 40L). Teflon tubing was used for the analyte, otherwise connections were made with Tygon tubing. The flow lines were terminated within the cell by glass nozzles which were rendered hydrophobic by immersion in dichlorodimethylsilane for 5 minutes. This treatment reduced the tendancy of drops to hang from the nozzles after solution delivery.

The cell was made from a 100 ml. round bottom pyrex flask to which a drain tube and solvent entry tube had been added (see Fig. 3). The original 24/40 ground glass joint was replaced by a screwtop and Teflon cap. Holes of the appropriate size were drilled in the cap for the electrodes and pump lines.

An argon gas line which was attached to the bottom of the cell at the same point as the drain tube served several functions. The purified argon completed deoxygenation of the solution and mixed it thoroughly. Furthermore, the churning of the solution removed any drops remaining on the pumpline nozzles and aided in cleaning of the cell during the wash cycle.

All valves were operated under computer control. The TTL levels available at the computer interface were used to switch a bank of relays and dual peripheral driver chips which provided the necessary voltage levels. The peripheral drivers (SN75450) were operated at 12V. The relays (Sigma 70R4) switched 115 VAC. The 24 VDC required by the relay coils was provided with SN7407 gates.

Electrodes and Potentiostat

The mercury electrode was constructed in-house and could automatically deliver stationary drops with a mass range which was adjustable between 0.8 and 15 mg. The drop mass used in this work was 3.7 mg. Assuming a spherical drop, the drop area was 0.02 cm^2.

The reference electrode was a saturated calomel fiber tipped electrode (Coleman 3-710). The electrode was lengthened and bent slightly for positioning within the cell.

A large spiral of platinum wire was used for the counter electrode. The spiral was 1.4 cm. in diameter. A large electrode was used to make the potential gradient in the solution as uniform as possible.

The electrode placement is shown in Figure 3. A Teflon spacer within the cell served to hold the electrodes in position. A glass rod not shown in the figure was connected to the spacer. This rod was shaken by an electromechanical arm to dislodge mercury drops from the electrode after use.

A relatively fast potentiostat was needed to monitor the charging current decay accurately. Such a potentiostat was constructed and is shown in Figure 4. All operational amplifiers were RCA 3140's. When a 10 mV step was applied to the potentiostat, the new potential (within 5%) was achieved at the reference after a period of 5 to 20 μsec, depending on the cell time constant.

The gain of the current measurement circuitry could be adjusted manually or under computer control. By changing the voltage at the FET gate, and by multiplexing the input and output of a 4X amplifier at the computer interface, the gain could be 1, 4, 8 or 32 times the manually

selected gain. Automatic gain control was necessary so that accurate measurements could be made on both the charging current and the Faradaic current within the same step.

The potentiostat, cell and solution mixing apparatus were all enclosed in a 32 x 22 x 18 inch acrylic box which was vented to a nearby hood. Aluminum sheet was fastened to the boxes' exterior so that it also served as a Faraday cage for noise reduction. An external high current relay was used to turn off all AC power within the box while measurements were being made.

Computer Hardware

A Hewlett Packard 2100S minicomputer with 32K words of core memory was used for generation of the staircase waveform, aquisition of data, and control of solution make-up. Peripherals included a general purpose interface, a paper tape punch and reader, a Tektronix 601 storage display monitor and a TRS-80 Model II computer used as an intelligent terminal. A 16 bit optically isolated digital to analog converter (DAC) was coupled to a sample and hold amplifier (SHM-1) for production of a clean staircase which was free from DAC switching noise. Analog to digital conversion was accomplished with an Analog Devices ADC-1103 converter and a SHA-IA S/H amplifier. Timing for all operations was derived from a 20 MHz crystal clock which was scaled to a frequency appropriate for the task being executed.

The 2100S was linked to a HP 2117F minicomputer which was faster and had more extensive mass storage and graphics capabilities. Peripherals of the 2117 included a 5 MByte disk, a Tektronics 4012 graphics terminal, a Centronics 306 printer and a Calcomp 565 digital plotter.

Experimental Timing

The staircase step height in all runs was 13.5 mV. The step length was adjusted to 13.5 or 54.0 msec. to produce scan rates of 1.00 and 0.25 V/s. 256 steps were made on each cyclic staircase, scanning a potential of 0.00 to -1.73 V. vs. S.C.E. 45 current measurements were made on each step. The first 41 were recorded at a rate of 100 KHz starting 31.4 microseconds after the step using direct memory access. The final four measurements were made under program control at times which were dictated by the scan rate. When the scan rate was 1.0 V/s the measurement times were 4.03, 4.13, 13.38 and 13.48 milliseconds after the step. At 0.25 V/s, the times were 16.18, 16.28, 53.88 and 53.98 msec.

Two independent scans were averaged for each voltammogram. Before averaging, the scans were compared to make sure that no random noise spikes were present. They were also checked for ADC overflow and for the absence of a current spike after a step which would indicate the absence of a mercury drop. Whenever an error condition was detected, the solution was bubbled with argon for a few seconds and the mercury electrode was sent through a self-cleaning routine, after which the voltammogram was retaken.

Experiments were performed in the order in which they are listed in Table 2. A new solution was created by adding components to the previous solution whenever possible. The cell was emptied and washed 3 times with deionized water after runs 5(a), 9, 13, and 16.

Hewlett Packard Basic was used to sequence the experiments and for operator I/O. Assembly subroutines were used for data aquisition and for all data manipulation done by the 2100 computer.

The 2100 computer sent the data block obtained from each experiment to the 2117 as soon as it was acquired. A FORTRAN program was run there to sort the Faradaic current from the data block and to calculate R_u and C_{dl}.

Faradaic Current Extraction

Current readings taken at the end of each step and at 30% of the step time were assumed to be predominantly Faradaic in nature. One of the two sampling times was selected as required by the factorial design. The two points which bracketed the desired time were averaged for signal to noise enhancement and stored in a permanent disk file.

Calculation of R_u and C_{dl}

The uncompensated resistance, R_u, and the double layer capacitance, C_{dl}, were calculated from the charging current decay data for each step. It was assumed that the Faradaic current remained constant over the time frame of the measurements and that it was equal to the current reading taken at the end of the previous step. Its contribution was subtracted from the charging current before further processing.

Taking the log of the familiar exponential decay equation allowed R_u and C_{dl} to be calculated by linear regression:

$$\log(i) = \log(\Delta V/R_u) - t/R_u C_{dl} \qquad (1)$$

An initial estimate of $R_u C_{dl}$, the cell time constant was made using only the 1st and 20th point taken after the step. Six points at evenly spaced intervals were then selected to cover 1 time constant and a second regression was done.

The time scale for the 2nd regression was constructed by considering the peak of the charging current spike to be at time zero. This corrected for the dependence of the potentiostat's risetime on the capacitance of the double layer. Since the peak was not contained within the data, it was estimated from the following equation:

$$t_{peak(microsec)} = 6.18 * C(uF) + 12.2 \qquad (2)$$

The 2-point estimate of C_{dl} was used in the equation. Oscilloscope measurements showed that this procedure gave peak times which were in error by no more than 2 microseconds for capacitances between 0.2 and 1.5 μF. Changes in R_u between 100 and 500 ohms had no effect on the peak time.

Blanks

A blank was recorded each time a new solution was made or the instrumentation was adjusted. Both the differential capacity blank and the Faradaic blank (primarily the reduction of water) were recorded, and at the operator's discretion could be subtracted from the corresponding responses when the analyte was present.

RESULTS AND DISCUSSION

Dummy Cell Measurements

The accuracy of the double layer capacity and uncompensated resistance measurements was evaluated with a series of 15 dummy cells having time constants between 67 and 921 microseconds. 2% plastic capacitors and 1% metal film resistors were used. The results are listed in Table 4. The standard error for R_u was 4.4 ohms and this error tended to be smaller for larger cell time constants. The standard error in C_{dl} estimation was 0.034 microfarads. It was relatively constant over the entire range of time constants examined.

Separation of Faradaic and Capacitive Currents

The accuracy of the dummy cell determinations can give an overly optimistic view of the error involved in double layer capacity measurements in real systems where Faradaic current is involved. Complete separation of Faradaic and capacitive currents can never be assumed (28, 29, 30). When trying to calculate the cell time constant from the step current decay, the presence of a rapid electron transfer reaction not only is an interference in itself, but it will also cause the flow of induced charging current which further complicates the calculation (31). Although simulation methods have been used to characterize the induced charging current caused by reversible electron transfer, no information is yet available for irreversible systems such as are being studied in this work.

The presence of Faradaic interference in differential capacity curves can be recognized by unusually high capacity values near a redox couples' $E_{1/2}$. This effect is shown for a solution of aniline and cadmium nitrate in KCl (Fig. 5). The shape of the curve agrees with literature values for the aniline-KCl system except for the potential region around -0.6 V vs. S.C.E. where an extraneous peak is found. No distortion is seen at potentials somewhat anodic of $E_{1/2}$ or at potentials where the cadmium reduction is diffusion controlled. Similar results were observed with iron oxalate.

An effort was made to separate reversible Faradaic and capacitive responses by a curve-fitting technique. It was postulated that the step current response at early times could be represented by the sum of an exponential decay equation and a quadratic polynomial function representing both the Faradaic current and the induced charging current. This was found to be true for theoretical data generated by digital simulation, but fits to experimental data were not so successful. Curve fitting reduced the error in the cadmium-aniline system by 60%.

Fortunately the Faradaic current had little effect on differential capacity curves for most of the irreversible systems examined. The kinetics of oxygen reduction are slow (32), and the presence or absence of oxygen in the aniline solution had no effect on the differential capacity measurements. Figure 6 shows both responses for 1-chloro-2-nitrobenzene. No pseudo-capacity peak was found in the region of the reduction potential, -0.5 V vs. S.C.E. The same behavior was seen for all compounds with one benzene ring and for five of the nitrodiphenyl ethers. Faradaic interference peaks were found in the differential capacity curves for Ethers 4, 6, 7 and 8 for the conditions of experiments 4 and 7 even though their reduction was irreversible. This is shown in Figure 7b. In such cases it is difficult to say whether

the peak was totally due to Faradaic current or if it was due in part to a true change in capacity caused by the electron transfer reaction. The fact that there is a change in the limiting capacity on either side of the peak supports the latter view.

The contribution of charging current to the Faradaic measurements was very small in most cases. The average R_u for solutions in which ethanol was at its high level was 509 ohms. When ethanol was at its low level, the average R_u was 386 ohms. Since the average double layer capacitance was 0.37 microfarads, the first sampling of the Faradaic current was typically made at 24 cell time constants after the step. At 24 cell time constants, both step charging current and induced charging current should be insignificant (31).

The only anomalous Faradaic current measurements were observed for three of the nitrodiphenylethers. Voltammograms of Ethers 1, 2, and 4 showed peaks which could not be explained by any reasonable Faradaic process (see Figure 7a). These peaks always occurred in regions where there was an abrupt change in differential capacity without a differential capacity peak, and thus could be attributed to a very slow adsorption-desorption process.

Variable Effects

If a change in the level of a variable is to yield information which is useful in qualitative analysis, the change must be large enough to produce a response from the analyte which is significantly larger than the experimental noise. It would also be advantageous if each variable had a unique effect on the analyte's response so that no redundant information is collected. A detailed analysis of variable effects is presented elsewhere (32). Here, we will consider results with two specific compounds: 1-chloro-2-nitrobenzene and ether 4.

The standard errors of the effects (34) for both the capacitive and Faradaic responses were calculated at each voltage for both compounds. The standard errors were then used to generate 95% confidence intervals which were superimposed on the plots of each effect. This is shown in Figure 8. 95% of all variations due to experimental noise will fall within the shaded region. Any excursion of an effect curve beyond the shaded region representing the confidence interval can be considered significant.

All variables had a significant effect on the Faradaic response for both 1-chloro-2-nitrobenzene and Ether 4. The magnitude of the effects decreased in the following order: pH > scan rate, ethanol, number of cycles > drop hang time > sampling time, surfactant. The shapes of all the effect curves were quite different for 1-chloro-2-nitrobenzene. For Ether 4, the effect of scan rate and drop hang time were similar, but still differed from each other by more than a microamp in some places. The same was true for the effects of pH and ethanol.

The only variables which had a significant effect on the capacitive response of 1-chloro-2-nitrobenzene were pH, number of cycles and ethanol. The effects of the number of cycles and pH were comparable in magnitude while the ethanol effect was much smaller. The shapes of each of the variable effect curves were different.

All of the variables except for the sampling time had a significant effect on the capacitive response of the strongly adsorbed Ether 4. (The sampling time variable applies only to Faradaic measurements.) The magnitude of the effects decreased in the following order: number of cycles > pH > scan rate ethanol > hang time > surfactant. None of the effect curves showed much similarity in shape.

Since a possible sampling time effect on determination of capacity can be eliminated on first principles, an estimate can be made of the size of 3 factor interactions. The ethanol-number of cycles-scan rate, ethanol-pH-surfactant, and the pH-number of cycles-hang time interactions were confounded among themselves, but were free from any lower order effects. The capacitive response to these interactions was not significant at any voltage. This justifies our earlier assumption that high order interactions can be ignored in calculating the main effects, at least for the capacitive responses.

CONCLUSIONS

The Faradaic and capacitive responses were determined accurately and independently for most of the compounds studied through the use of the cyclic staircase waveform. Very fast electron transfer and very slow adsorption-desorption occasionally degraded the separation of the two responses. Comparisons between the differential capacity curves and the voltammograms were helpful in identifying situations in which a Faradaic response could be mistaken for a capacitive response and vice versa.

The variables chosen and the levels over which they were changed appeared to be appropriate for later pattern recognition analysis. The changes in all the experimental variables were large enough and reproducible enough to produce significant effects on both the Faradaic and capacitive responses of an analyte. The effect of each variable was unique, so that redundant information was not recorded.

The methodology described here appears to provide a convenient, reliable means of generating an electrochemical data base appropriate for qualitative characterization of organic analytes. The information content appears to be large. Subsequent pattern recognition studies will be reported to demonstrate applicability to computerized analyte classification.

ACKNOWLEDGEMFNT

The authors express gratitude for the support of the Office of Naval Research.

REFERENCES

1. Zuman, P. "The Elucidation of Organic Electrode Processes"; Academic Press: New York, 1969; p 123.
2. Wopschall, R. H.; Shain, I. Anal. Chem. 1967, 39, 1514.
3. Peover, M. E.; Powell, J. S. J. Electroanal. Chem. 1969, 20, 427.
4. Krygowshi, T. M.; Stencel, M.; Galus, Z. J. Electroanal. Chem. 1972, 39, 395.
5. Sybrandt, L. B.; Perone, S. P. Anal. Chem. 1972, 44, 2331.
6. Thomas, Q. V.; DePalma, R. A.; Perone, S. P. Anal. Chem. 1977, 49, 1376.
7. DePalma, R. A.; Perone, S. P. Anal. Chem. 1979, 51, 829.
8. Schachterle, S. D.; Perone, S. P. Anal. Chem. 1981, 53, 1672.
9. Meites, L.; Zuman, P.; Rupp, E.; Fennor, T.; Spritzer, L. "CRC Handbook in Organic Electrochemistry", CRC Press: Boca Raton, Florida, 1978; Vol. 1-4.
10. Burgard, D. R.; Perone, S. P. Anal. Chem. 1978, 50, 1366.
11. Yih, R. Y.; Swithenbank, C. J. Agr. Food Chem. 1975, 23, 592.
12. Damaskin, B. B.; Petrii, O. A.; Balrakov, V. V. "Adsorption of Organic Compounds on Electrodes", Plenum Press: New York, 1971; p. 40.
13. Amadelli, R.; Daghetti, A.; Vergano, L.; DeBattisti, A.; Trasatti, S. J. Electroanal. Chem. 1979, 100, 379.
14. Damaskin, p. 39.
15. Gupta, S.; Sharma, S. Electrochim. Acta 1965, 10, 151.
16. Dutkiewicz, E.; Puacz, A. J. Electroanal. Chem. 1979, 100, 947.
17. Bockris, J. O'M.; Reddy, A. K. N. "Modern Electrochemistry"; Plenum Press: New York, 1970; p 714.

18. Valeriate, E. M. C.; Barradas, R. G. J. Electroanal. Chem. 1966, 12, 67.

19. Barradas, R. G.; Kimmerle, F. M. J. Electroanal. Chem. 1965, 9, 483.

20. Retajczyk, T. F.; Roe, D. E. J. Electroanal. Chem. 1968, 16, 21.

21. Pilla, A. A.; Margules, G. S. J. Electrochem. Soc. 1977, 124, 1697.

22. Ichise, M.; Yamagishi, H.; Oishi, H.; Kojima, T. J. Electroanal. Chem. 1980, 106, 35.

23. Elkin, V. V.; Leutsner, B. I.; Abaterov, M. A.; Kuzmin, V. G. J. Electroanal. Chem. 1979, 96, 143.

24. Ryan, M. D. J. Electroanal. Chem. 1977, 79, 105.

25. Zipper, J. J.; Perone, S. P. Anal. Chem. 1973, 45, 452.

26. Hendrix, C. D. CHEMTEC 1979, 9, 167.

27. G. E. P. Box, Hunter, W. G.; Hunter, J. S. "Statistics for Experimenters"; John Wiley and Sons: New York, 1978; Chapter 12.

28. Delahay, P. J. Phys. Chem. 1966, 70, 2373.

29. Pilla, A. A. in "Electrochemistry, Calculations, Simulation and Instrumentation", Mattson, Mark and MacDonald, Ed.; Marcel Dekker: New York, 1972.

30. Fratoni, S. S. Jr.; Perone, S. P. Anal. Chem. 1976, 48, 287.

31. Miaw, L. L.; Perone, S. P. Anal. Chem. 1979, 51, 1645.

32. Delahay, P. "Double Layer and Electrode Kinetics"; Wiley-Interscience: New York, 1965; Chapter 10.

33. Byers, W. A.; Freiser, B. S.; Perone, S. P., submitted to Anal. Chem.

34. G. E. P. Box, Hunter, W. G.; Hunter, J. S. "Statistics for Experimenters"; John Wiley and Sons: New York, 1978; p 319.

TABLE 1. Variable Levels

VARIABLE NUMBER	VARIABLE	LOW LEVEL (-)	HIGH LEVEL (+)
X_1	% Ethanol	0.5 %	9.5 %
X_2	pH	8.0	5.1
X_3	Surfactant Concentration	0	1.4×10^{-5} M
X_4	Number of Cycles	1	2
X_5	Scan Rate	0.25 V/s.	1.0 V/s.
X_6	Drop Hang Time	0.2 s.	30 s.
X_7	Sampling Time	30% of step (α'=.7)	end of step (α'=.007)

TABLE 2. Fractional Factorial Design

Experiment	Variable						
	X_1	X_2	X_3	X_4	X_5	X_6	X_7
1	+	-	-	-	-	+	+
2	+	-	-	+	+	-	+
3	+	+	-	+	-	-	-
4	+	+	-	-	+	+	-
5(a)	+	+	+	+	+	+	+
6	-	-	+	+	-	-	+
7	-	-	+	-	+	+	+
8	-	+	+	-	-	+	-
9	-	+	+	+	+	-	-
10	-	-	-	+	+	+	-
11	-	-	-	-	-	-	-
12	-	+	-	-	+	-	+
13	-	+	-	+	-	+	+
14	+	-	+	-	+	-	-
15	+	-	+	+	-	+	-
5(b)	+	+	+	+	+	+	+
16	+	+	+	-	-	-	+

TABLE 3. Compounds Studied

Nitrobenzenes

1. p-nitrophenol
2. 1-chloro-2-nitrobenzene
3. o-nitrophenol
4. m-nitrophenol
5. m-nitrotoluene
6. 1-chloro-4-nitrobenzene
7. p-nitrotoluene
8. 2-6-dichloro-4-nitrophenol
9. p-nitroanisole
10. α-chloro-m-nitrotoluene

Nitrodiphenylethers

1. 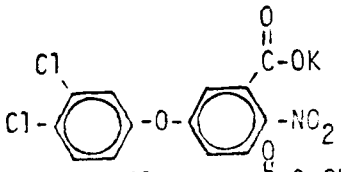
2. 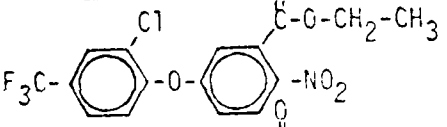
3. 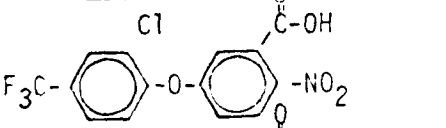
4. 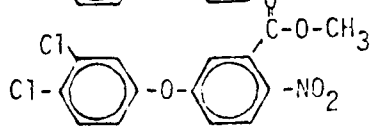
5. 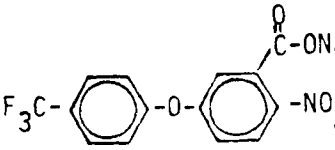
6. 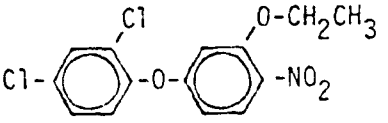
7. 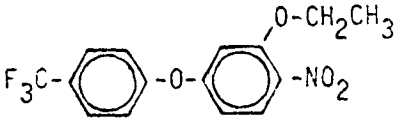
8. 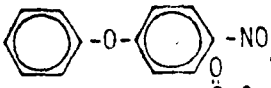
9. 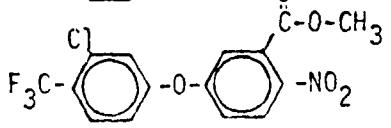

TABLE 4. Dummy Cell Results

Cell #	Ru		Cdl	
	True	Experimental	True	Experimental
1	175	183	.382	.35
2	175	180	.765	.71
3	175	180	1.15	1.10
4	175	179	1.53	1.51
5	175	176	2.29	2.23
6	301	305	.382	.35
7	301	306	.765	.76
8	301	303	1.15	1.13
9	301	303	1.53	1.50
10	301	302	2.29	2.26
11	402	410	.382	.36
12	402	405	.765	.77
13	402	401	1.15	1.12
14	402	400	1.53	1.50
15	402	399	2.29	2.28

LIST OF FIGURES

Figure 1. (a) Elkin's semitrapazoidal waveform (b) Staircase waveform. (c) Current response to staircase. Shaded portion shows time during which capacitance data are taken. X's show timing of Faradaic measurements.

Figure 2. Solvent delivery system.

Figure 3. Cell design.

Figure 4. Potentiostat design.

Figure 5. 0.05M aniline and 8 x 10^{-5}M $Cd(NO_3)_2$ in 1.0M KCl.

Figure 6. 1-chloro-2-nitrobenzene response in experiment #1. (a) Current. (b) Differential Capacity.

Figure 7. Response of Ether #4 in experiment #4. (a) Current. (b) Differential capacity. Peaks number 3 and 4 in graph (a) are due to capacitive effects. The sharp peak in graph (b) has both a capacitive and Faradaic component.

Figure 8. The effect of ethanol on the Faradaic response of 1-chloro-2-nitrobenzene. The shaded region represents the confidence interval for the effect. The effect curve is the average change in a staircase voltammogram when the percentage of ethanol in solution is changed from 9.5 to 0.5%.

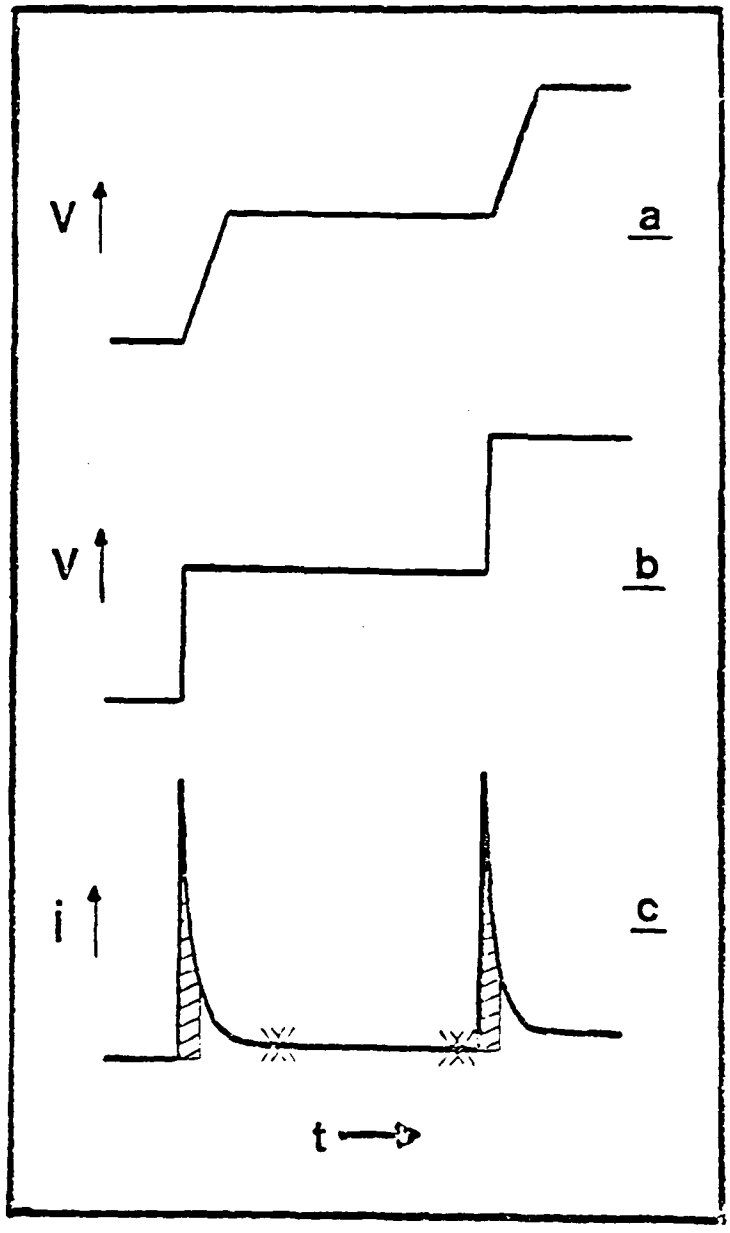

Figure 1.

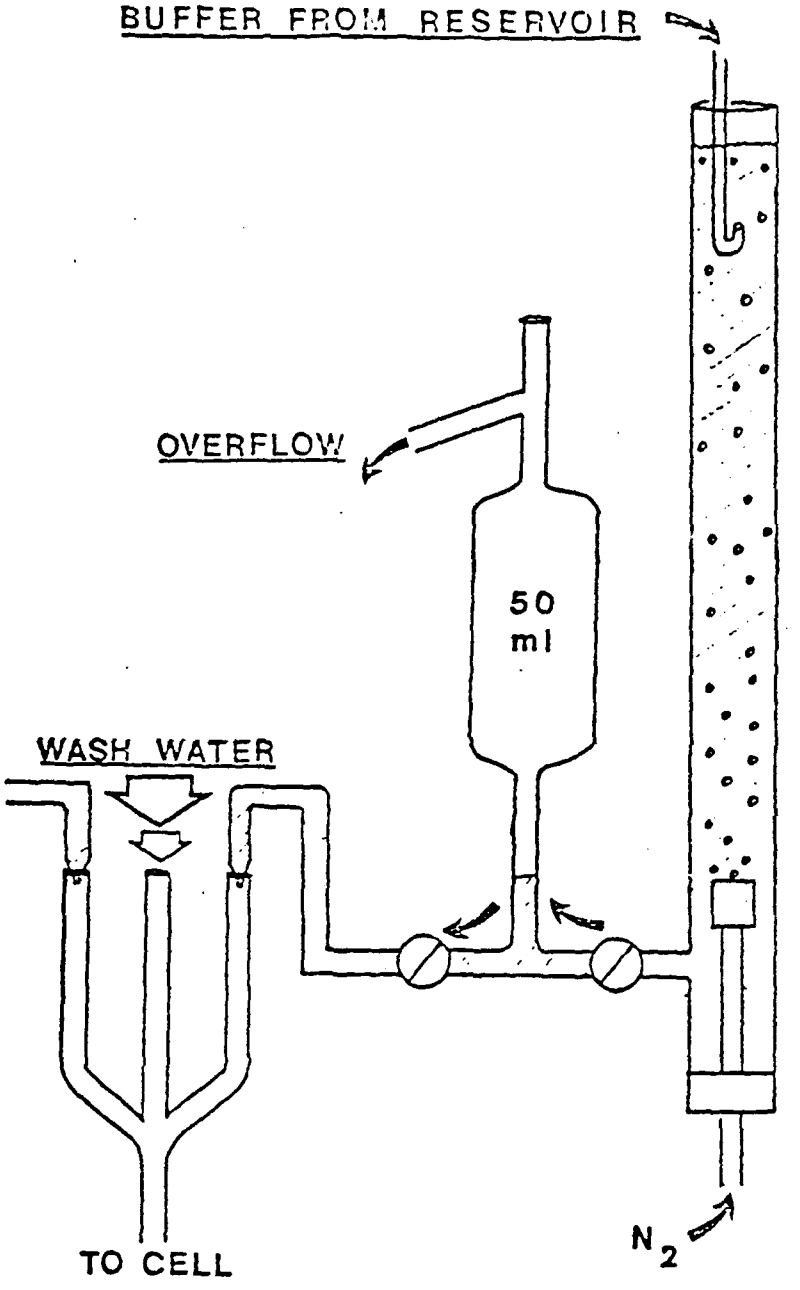

Figure 2. Solvent delivery system.

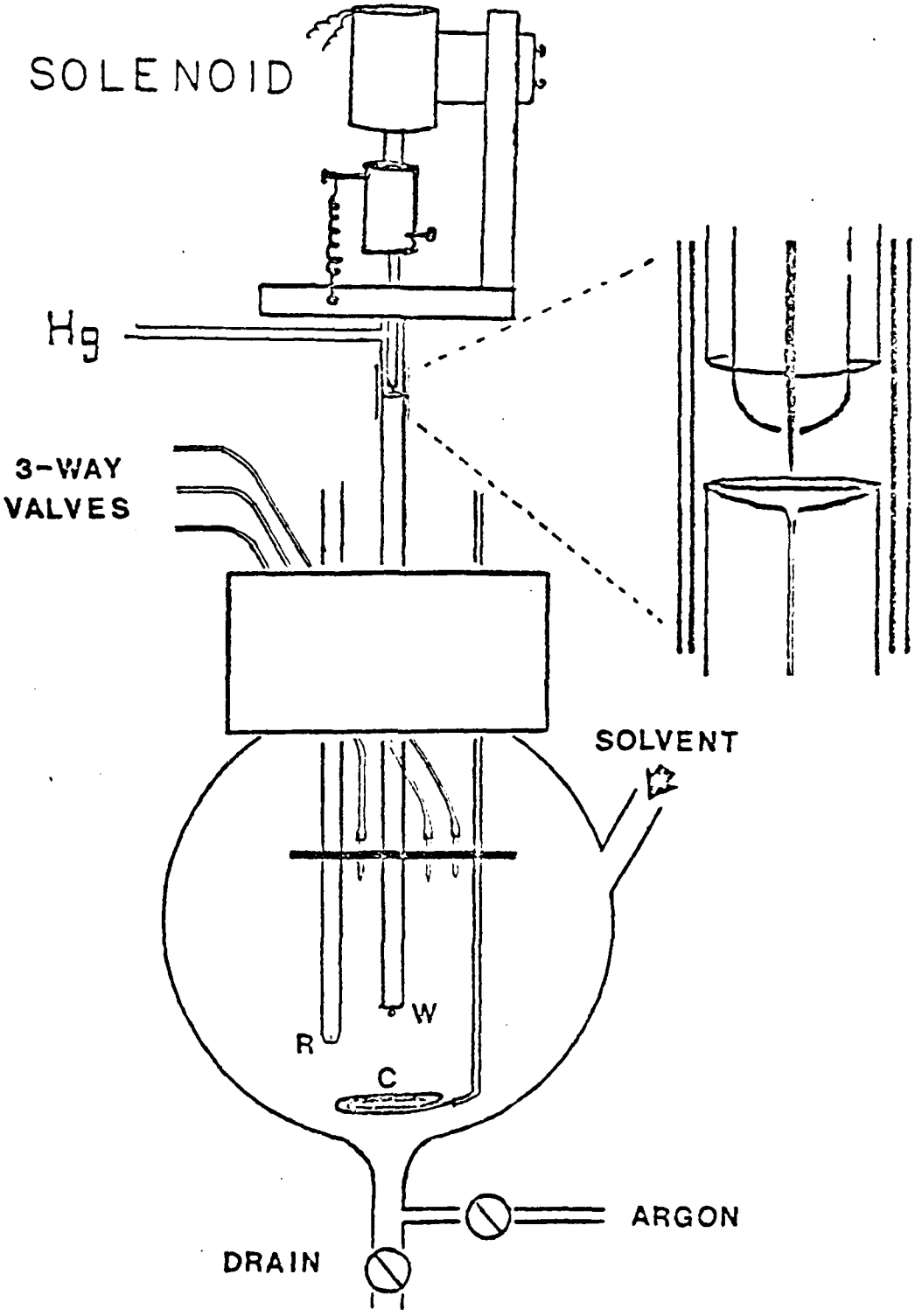

Figure 3. Cell Design.

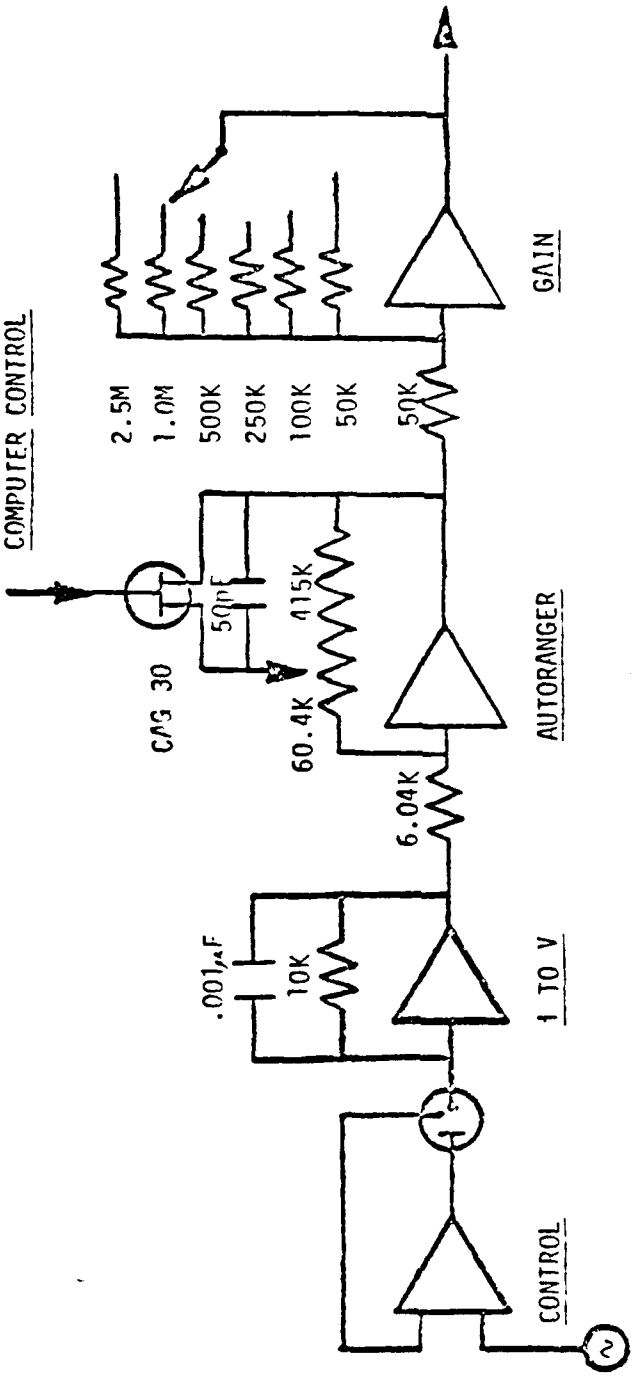

Figure 4. Potentiostat design.

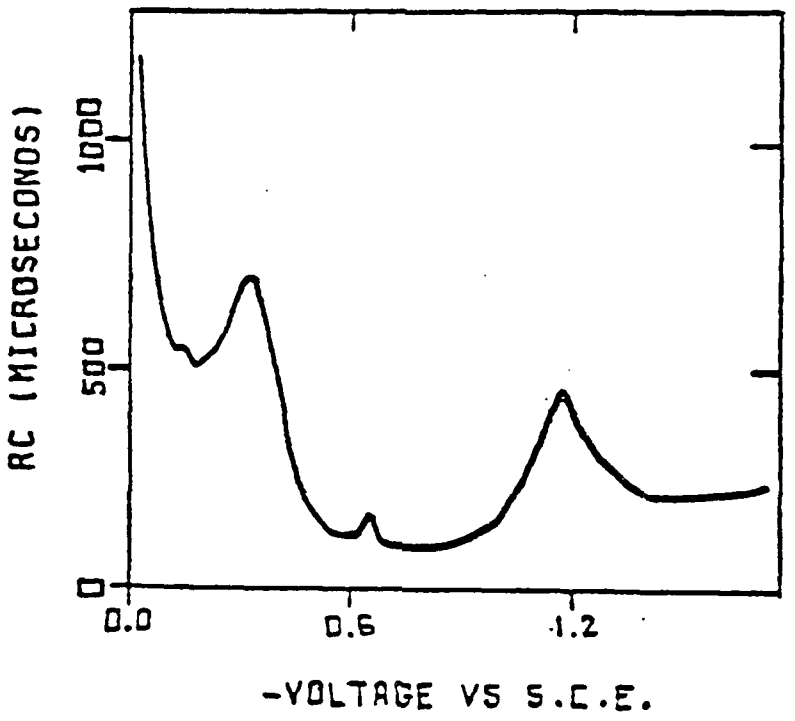

Figure 5. 0.05M aniline and 8 x 10^{-5}M $Cd(NO_3)_2$ in 1.0M KCl.

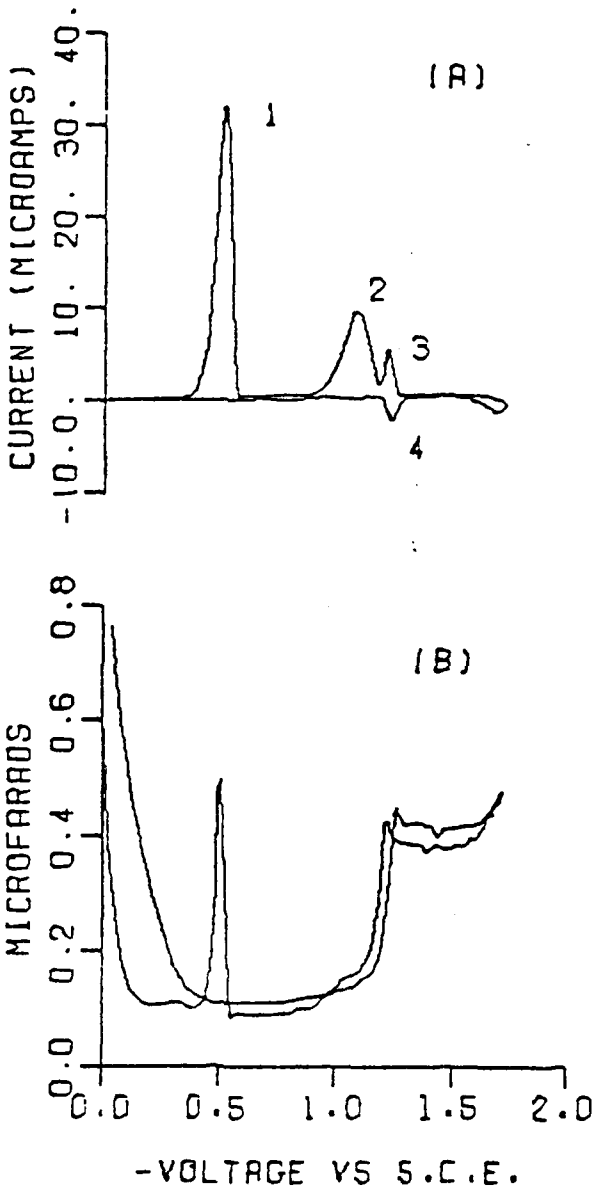
(A)
CURRENT (MICROAMPS)
-10.0. 10. 20. 30. 40.
1
2
3
4
(B)
MICROFARADS
0.0 0.2 0.4 0.6 0.8
0.0 0.5 1.0 1.5 2.0
-VOLTAGE VS S.C.E.

Figure 6.

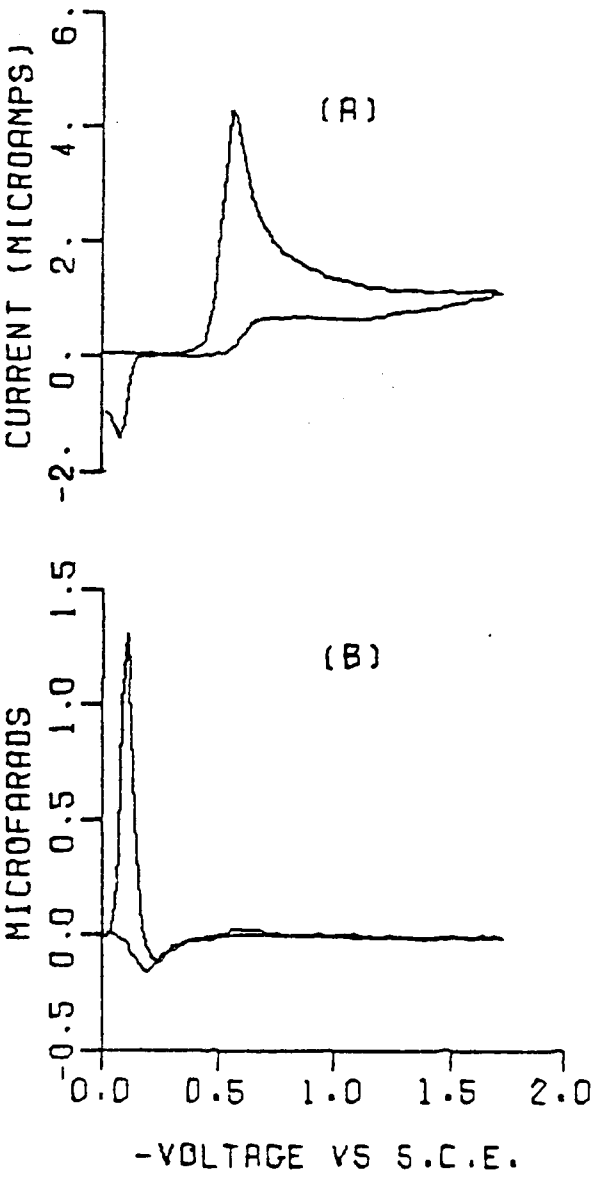
CURRENT (MICROAMPS)
6.
4.
2.
0.
-2.
(A)
MICROFARADS
1.5
1.0
0.5
0.0
-0.5
(B)
0.0
0.5
1.0
1.5
2.0
-VOLTAGE VS S.C.E.

Figure 7.

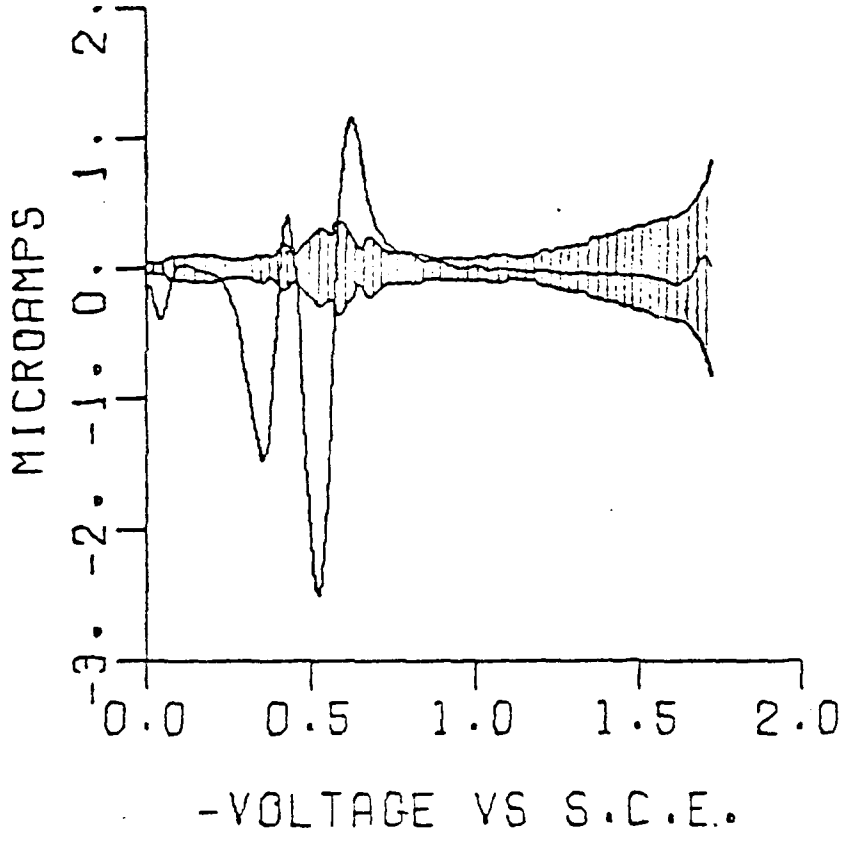

Figure 8.

TECHNICAL REPORT DISTRIBUTION LIST, GEN

	No. Copies
Office of Naval Research Attn: Code 472 800 North Quincy Street Arlington, Virginia 22217	2
ONR Branch Office Attn: Dr. George Sandoz 536 So. Clark Street Chicago, Illinois 60605	1
ONR Branch Office Attn: Scientific Dept. 715 Broadway New York, New York 10003	1
ONR Branch Office 1030 East Green Street Pasadena, California 91106	1
ONR Branch Office Attn: Dr. L. H. Peebles Building 114, Section D 666 Summer Street Boston, Massachusetts 02210	1
Director, Naval Research Laboratory Attn: Code 6100 Washington, D.C. 20390	1
The Assist Secretary of the Navy (R,E&S) Department of the Navy Room 4E736, Pentagon Washington, D.C. 20350	1
Commander, Naval Air Systems Command Attn: Code 310C (H. Rosenwasser) Department of the Navy Washington, D.C. 20360	1
Defense Documentation Center Building 5, Cameron Station Alexandria, Virginia 22314	12
Dr. Fred Saalfeld Chemistry Division Naval Research Laboratory Washington, D.C. 20375	1
U.S. Army Research Office Attn: CRD-AA-IP P.O. Box 1211 Research Triangle Park, N.C. 27709	1
Naval Ocean Systems Center Attn: Mr. Joe McCartney San Diego, California 92152	1
Naval Weapons Center Attn: Dr. A. B. Amster, Chemistry Division China Lake, California 93555	1
Naval Civil Engineering Laboratory Attn: Dr. R. W. Drisko Port Hueneme, California 93401	1
Department of Physics & Chemistry Naval Postgraduate School Monterey, California 93940	1
Dr. A. L. Slafkosky Scientific Advisor Commandant of the Marine Corps (Code RD-1) Washington, D.C. 20380	1
Office of Naval Research Attn: Dr. Richard S. Miller 800 N. Quincy Street Arlington, Virginia 22217	1
Naval Ship Research and Development Center Attn: Dr. G. Bosmajian, Applied Chemistry Division Annapolis, Maryland 21401	1
Naval Ocean Systems Center Attn: Dr. S. Yamamoto, Marine Sciences Division San Diego, California 91232	1
Mr. John Boyle Materials Branch Naval Ship Engineering Center Philadelphia, Pennsylvania 19112	1

TECHNICAL REPORT DISTRIBUTION LIST, GEN

	No. Copies
Dr. Rudolph J. Marcus Office of Naval Research Scientific Liaison Group American Embassy APO San Francisco 96503	1
Mr. James Kelley DTNSRDC Code 2803 Annapolis, Maryland 21402	1

TECHNICAL REPORT DISTRIBUTION LIST, 051C

	No. Copies
Dr. M. B. Denton Department of Chemistry University of Arizona Tucson, Arizona 85721	1
Dr. R. A. Osteryoung Department of Chemistry State University of New York at Buffalo Buffalo, New York 14214	1
Dr. B. R. Kowalski Department of Chemistry University of Washington Seattle, Washington 98105	1
Dr. D. L. Venezky Naval Research Laboratory Code 6130 Washington, D.C. 20375	1
Dr. H. Freiser Department of Chemistry University of Arizona Tucson, Arizona 85721	1
Dr. Fred Saalfeld Naval Research Laboratory Code 6110 Washington, D.C. 20375	1
Dr. P. Chernoff Department of Mathematics Massachusetts Institute of Technology Cambridge, Massachusetts 02139	1
Dr. [illegible] Department of Chemistry University of California, San Diego La Jolla, California 92037	1
Dr. A. Zirino Naval Undersea Center San Diego, California 92132	1
Dr. John Duffin United States Naval Postgraduate School Monterey, California 93940	1
Dr. G. M. Hieftje Department of Chemistry Indiana University Bloomington, Indiana 47401	1
Dr. Victor L. Rehn Naval Weapons Center Code 3813 China Lake, California 93555	1
Dr. Christie G. Enke Michigan State University Department of Chemistry East Lansing, Michigan 48824	1
Dr. Kent Eisentraut, MBT Air Force Materials Laboratory Wright-Patterson AFB, Ohio 45433	1
Walter G. Cox, Code 3632 Naval Underwater Systems Center Building 148 Newport, Rhode Island 02840	1
Dr. George Morrison Department of Chemistry Cornell University Ithaca, New York 14850	1
Dr. Isiah M. Warner Department of Chemistry Texas A&M University College Station, Texas 77840	1